Design to Improve Starting Performance of Line-Start Synchronous Reluctance Motor for Household Appliances

H. Nam, S. B. Park, G. H. Kang, and J. P. Hong
Dept. of Electrical Engineering
Changwon National University
Changwon, Gyeongnam, Korea, 641-773
haeggee@korea.com

J. B. Eom, and T. U. Jung
Digital Appliance Company Research Lab.
LG Electronics Inc.
Changwon, Gyeongnam, Korea, 641-711
tujung@lge.com

Abstract— **A single-phase line-start synchronous reluctance motor (LsynRM) has merits of low cost, high efficiency, and reliability. The LSynRM has the unbalanced magnetic circuit caused by flux barriers and various shapes of conductor bars. Thus, the motor can cause the unbalanced starting torque with the initial starting position of the rotor This paper presents the design to improve starting performance of the LSynRM for household appliances. Design variables are the number and the shape of the conductor bars. The motor is analyzed by finite element (FE) analysis. A SPIM (Single-phase induction motor) for mass production, a prototype, and a designed model of LSynRM are manufactured and tested.**

Keywords- Line-start synchronous reluctance motor (LSynRM), unbalanced starting torque, initial starting position, flux barriers, finite element (FE) analysis.

I. INTRODUCTION

Over the past years, awareness of environmental problems has been grown dramatically and worldwide, and tremendous interest has been grown in developing the energy conversion technology. In household appliances, manufacturers are trying to improve the efficiency [1].

A capacitor-run single-phase induction motor (SPIM) is widely used in household appliances because of the direct operation by supplying the commercial single-phase voltage source. However, there is difficulty in improving efficiency because the resistance and the induced current in conductor bars cause the conductor bar loss [2].

On the other hand, a single-phase line-start permanent magnet synchronous motor (LSPMSM) has both a rotor cage for induction starting and permanent magnets (PMs) for synchronous torque. Since the motor operates as a synchronous machine in the steady-state, the rotor joule loss is significantly reduced [3]

Therefore, it is possible to achieve efficiency improvement in comparison with the SPIM. Yet the instantaneous starting current can lead the deterioration of motor performance as well as the irreversible demagnetization of PMs [4].

A single-phase line-start synchronous reluctance motor (LSynRM) does not need PMs contrary to the LSPMSM. Its rotor has conductor bars and flux barriers.

With the help of an induction cage, as shown in Fig. 1, the motor starts asynchronously. When the motor reaches synchronous speed, the reluctance torque by flux barriers, which cause the difference in d-axis inductance (L_d) and q-axis inductance (L_q), becomes the sole source and operates as a synchronous motor in steady-state.

Accordingly, the LSynRM is capable of efficiency improvement without cost rise compared with the SPIM. Most of all, the LSynRM can be independent to the demagnetization field, and the drop ratio in efficiency of the LSynRM is smaller than that of the LSPMSM. Therefore, the LSynRM can improve the reliability contrary to the LSPMSM. Still, unless high saliency ratio (L_d/L_q) and high inductance difference (L_d-L_q) are reached, torque density, power factor, and efficiency are low in the steady-state [5].

To increase L_d/L_q and L_d-L_q, the d-axis flux path should be obtained sufficiently. Consequently, q-axis conductor bars should be reduced. In contrast, d-axis conductor bars should be increased to reduce the conductor bar loss by the unbalanced rotating magnetic field.

However, with flux barriers, the various shapes of the conductor bars can cause the unbalanced starting torque according to the initial starting position of the rotor.

In this paper, the starting torque is defined as the induction torque at zero speed and it is expected that the LsynRM can have difficulty in starting according to rotor positions. Therefore, to improve the starting performance of the LsynRM, the number and the shape of the conductor bars are set as design variables and the starting performance by design variables are analyzed [6].

The process of the analysis is as follows.

Firstly, the number of the conductor bars is decided for uniform starting torque with the initial starting position.

0-7803-8487-3/04/$20.00 (C) 2004 IEEE

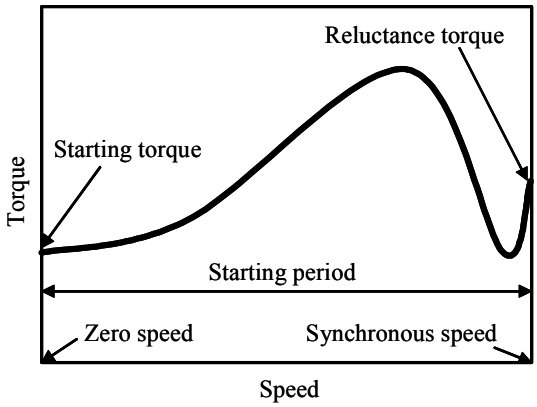

Figure 1. Torque vs. speed of LSynRM

Secondly, starting torque is analyzed according to the shape of the bars. Then, the effect of the flux barriers is analyzed when the number of the flux barriers is 3.

Lastly, the shapes of the conductor bars are designed to satisfy the uniform starting torque with initial starting position, and improve the efficiency in the steady-state.

A SPIM for mass production, a prototype, and a designed model of the LSynRM are manufactured and tested.

II. Structure and Characteristics of LSynRM

Fig. 2 shows the cross-section of the LSynRM.

The total number of the slots in the stator is 24, and main and auxiliary windings are inserted in each slot. The symbols, "M" and "A" represent the main winding and the auxiliary winding, respectively. These windings are displaced from each other by 90 electrical degrees in space around the air-gap circumference. In the rotor, there are several flux barriers for the reluctance torque, and conductor bars for the induction torque.

Fig. 3 displays the connection of stator winding of the LSynRM. The time-phase displacement between two winding currents is obtained by means of a capacitor C_R in series with the auxiliary winding. The capacitor is also used to improve the starting and the running performances of the motor, depending on the size and connection of the capacitor.

Table I represents the brief characteristics of the LSynRM. As shown in the table, the motor has both the induction torque by conductor bars and the reluctance torque by flux barriers.

Because of the flux barriers generating the reluctance torque, the magnetic circuit becomes unbalanced and the unbalanced magnetic circuit has a bad influence on the induction torque. As the results, the conductor bars of the motor can induce the unbalanced starting torque according to the initial starting position of the rotor.

The conductor bars generating the induction torque make it difficult to obtain sufficient L_d-L_q and L_d/L_q.

Therefore, it is very important to design the conductor bars and the flux barriers considering both the induction torque and the reluctance torque.

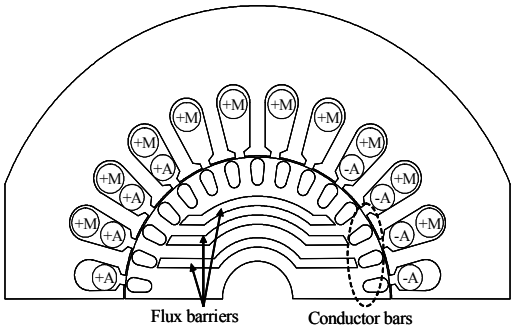

Figure 2. Cross-section of LSynRM.

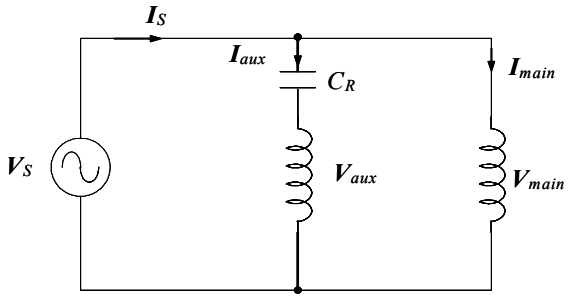

Figure 3. Stator winding connection of LSynRM.

TABLE I. Brief Characteristics of LSynRM

Item	Induction torque	Reluctance torque
Principle	Conductor bars at asynchronous speed	Flux barriers at synchronous speed
Requirement	Uniform starting torque with initial rotor starting position	Increase d-axis flux and minimize q-axis flux to obtain L_d-L_q and L_d/L_q
Problems	Difficulty in uniform starting toque with initial rotor position by flux barriers	Difficulty in L_d and L_q by conductor bars

III. Conductor Bar Design

A. Decision of the Number of the Conductor Bars

In the case of the induction motor having the squirrel-cage rotor, the slot combination of the stator and the rotor affects the starting characteristics, even though the motor has not the flux barriers. Therefore, it is very important to decide the number of the conductor bars.

Fig. 4 shows the analysis models according to the number of the conductor bars, which is 30, 32, 33, and 34, respectively. It is assumed that the models have same magnetic material, shape, and dimension. The analysis models do not have flux barriers, and the conductor bar resistances are uniform to avoid the difference of the torque magnitude. The skew effect is not considered in this paper.

When the rotor positions shown in Fig. 4 is defined as initial starting position of zero, each of the position is degree for starting from the zero speed, the analysis is performed from zero to eight with four-degree intervals.

Fig. 5 and Fig. 6 are results of the starting torque analysis results by the finite element (FE) analysis with the number of the conductor bars and the initial starting position, when the speed is zero.

As shown in the figures, the starting torque with 30 and 32 bars varies severely, whereas the torque with 33 bars has almost uniform value. The torque variation with 34 bars is smaller than that with 32 bars and is a little bit larger than that with 33 bars. In the case of the LSynRM, an even number of the conductor bars is suitable because the motor requires the symmetric magnetic circuit. Thus, the rotor of the LSynRM has 34 bars in this paper.

B. Torque Characteristics by the Shape of the Conductor Bars

Fig. 7 presents the analysis models having the various shapes of the conductor bars and the zero initial starting position.

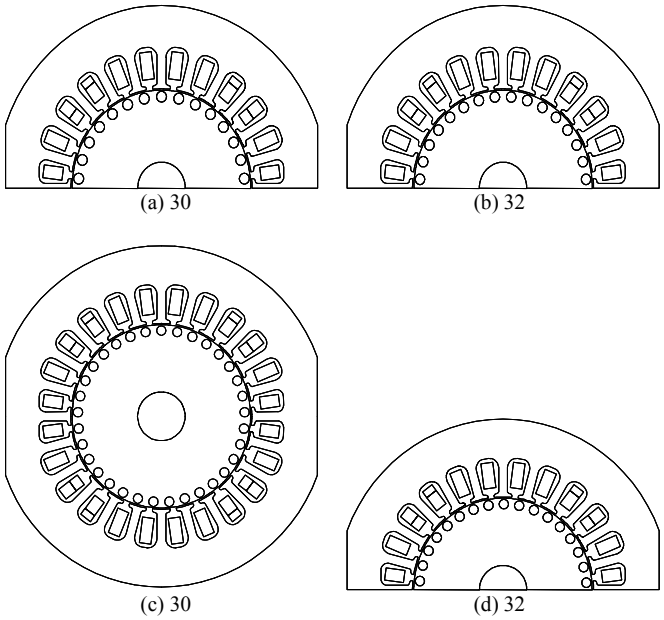

(a) 30 (b) 32

(c) 30 (d) 32

Figure 4. Analysis models with the number of conductor bars.

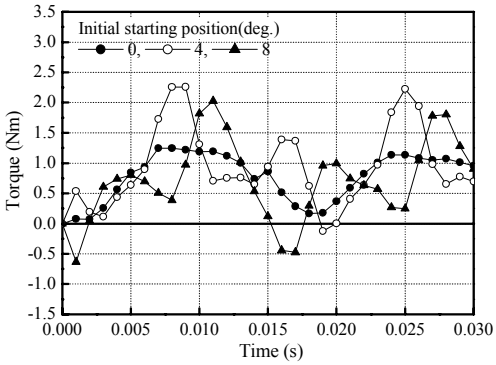

(a) 30

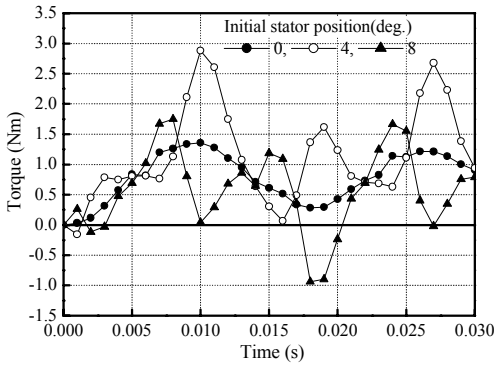

(b) 32

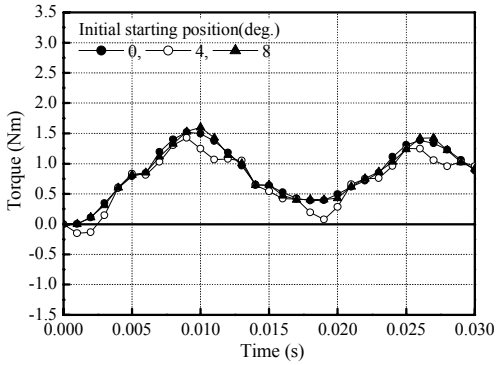

(c) 33

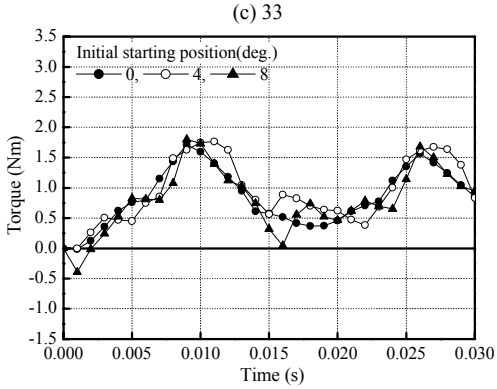

(d) 34

Figure 5. Instantaneous starting torques with the number of conductor bars and the initial rotor position at zero speed.

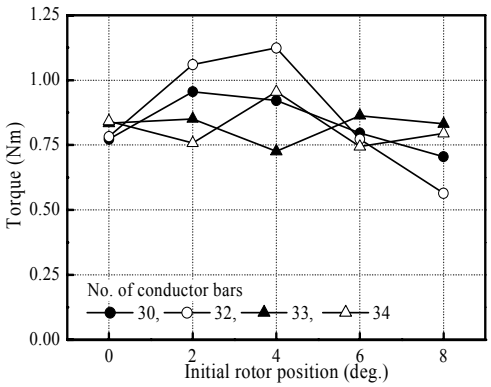

Figure 6. Average torques of the instantaneous starting torques in Fig. 5.

The models have 34 conductor bars and 3 flux barriers. d-axis conductor bars are numbered from the center of d-axis in counterclockwise (CCW) direction. In the same manner, q-axis conductor bars are numbered from the center of q-axis in CCW direction. Flux barriers are numbered from the shaft in radial direction.

When the shape of the conductor bars varies in order, the motor does not have flux barriers. In other words, the motor operates as a SPIM. On the other hand, when the motor has flux barriers, conductor bars have equal shapes.

When the models have the same shape of the conductor bars without the flux barriers shown in Fig. 7, the average starting torques by FE analysis is shown in Fig. 8. The analysis is performed in ten-degree intervals from 0 deg. to 180 deg..

The torque, 0.65 Nm is normalized as 100 %.

As shown in Fig. 8, it is confirmed that the models, as induction motors, have a good self-start capability.

Fig. 9 displays the average starting torques with the shape of the conductor bars and the flux barriers.

From the left hand to the right hand, the values of the horizontal axis are named as Ref, Bard_1, Bard_2, Bard_3, Bard_4, Barq_1, Bar_q2, Barq_3, Barq_4, Barq_5, Barr_1, Barr_2, and Barr_3 in order. "Ref" means the SPIM which has uniform conductor bars. "Bard", "Barq", and "Barr" mean the d-axis bar, the q-axis bar, and the flux barrier, respectively. The area of the changed bar is twice larger than that of the original bar.

The values of the vertical axis are the normalized torque.

Provided that No. 1 of the d-axis bar is increased, the bar causes negative starting torque at 70 deg., even though the bar increases starting torque at that of 80 deg.

On the contrary to the No. 1 of the d-axis bar, that No. 2 of the d-axis bar is increased, the bar induces negative starting torque at 80 deg., though the bar increases starting torque at the initial starting position of 70 deg..

When No. 2 of the q-axis bar is increased, the bar reduces the starting torque at 10 and 20 deg..

The flux barriers of No. 1, and No. 2 have an bad influence on the initial starting position of 70, 100, and 120 deg..

The rest of the conductor bars and the flux barriers also show the similar characteristics. Therefore, it is very important to design flux barriers, and, especially, conductor bars for a good starting performance from uniform starting torque with the initial starting position.

IV. Design and Analysis Results

Fig. 10 and Table II show the cross-section and the brief specifications of a prototype and a designed model of the LsynRM, respectively.

Two kinds of models have identical stators. The stator lamination, stack length, winding's effective turns are the same. The rotors of the models are different. While the prototype has 32 bars and 5 flux barriers, the designed model has 34 bars and 3 flux barriers. k_w, the ratio of flux barrier width to iron sheet rib width, of the former is 0.67, and that of the latter is 0.74. The resistance of the conductor bars of the designed model is larger than that of the prototype, as shown in Table II.

The shapes of the conductor bar of the designed model are determined using Fig. 8, and normalized area of each conductor bar is shown in Fig. 11.

Fig. 12 indicates average starting torques of the prototype and the designed model. In Fig. 12(a), the prototype has negative starting torque positions. Unlike this, the designed model generates positive starting torque all over the initial starting positions even though the starting torques between 30 deg. and 130 deg. are smaller than in other degrees.

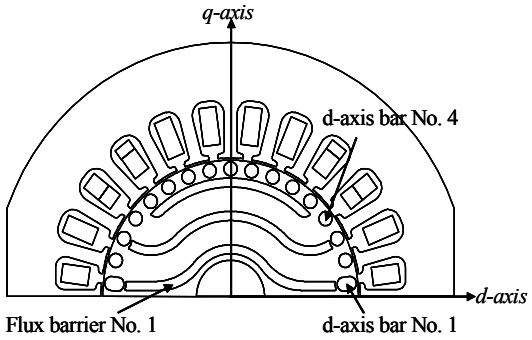

(a) d-axis conductor bars and flux barriers

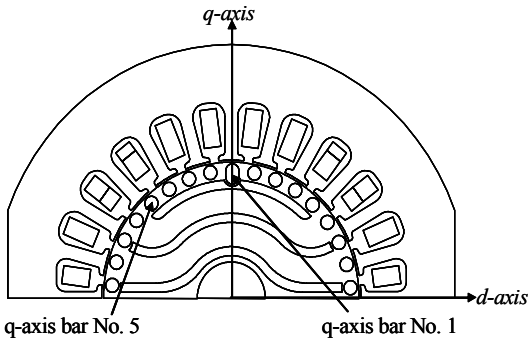

(b) q-axis conductor bars

Figure 7. Analysis models with the shape of conductor bars.

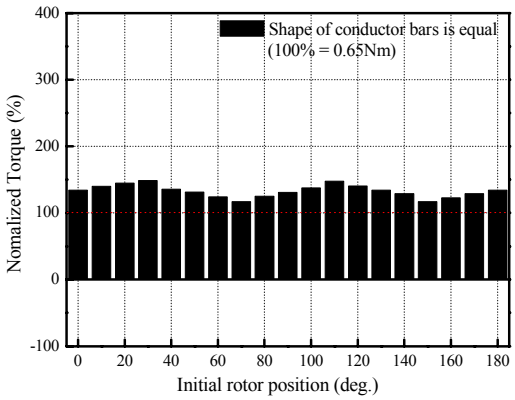

Figure 8. Average starting torques when the analysis models in Fig. 7 are operated as induction motors.

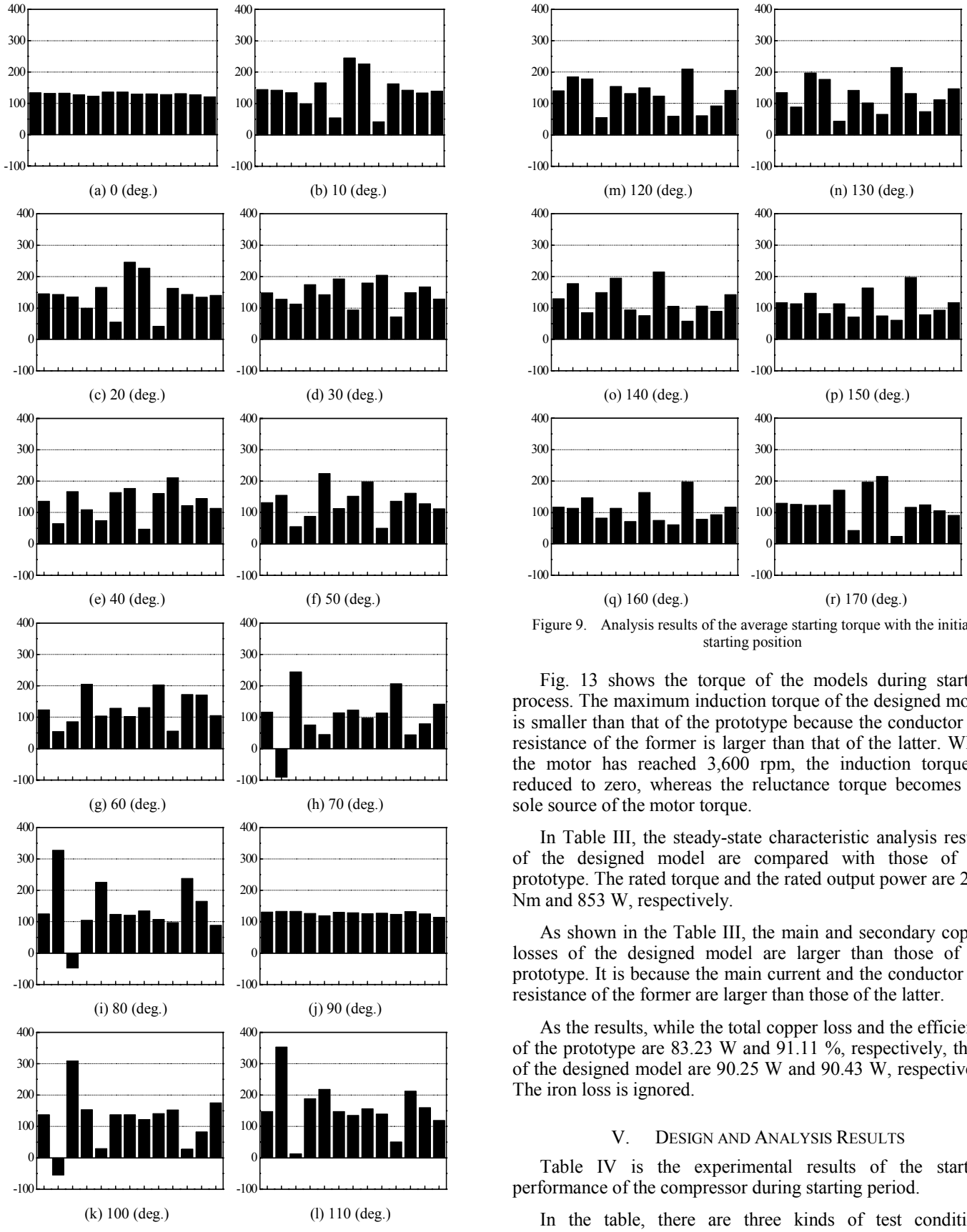

Figure 9. Analysis results of the average starting torque with the initial starting position

Fig. 13 shows the torque of the models during starting process. The maximum induction torque of the designed model is smaller than that of the prototype because the conductor bar resistance of the former is larger than that of the latter. When the motor has reached 3,600 rpm, the induction torque is reduced to zero, whereas the reluctance torque becomes the sole source of the motor torque.

In Table III, the steady-state characteristic analysis results of the designed model are compared with those of the prototype. The rated torque and the rated output power are 2.26 Nm and 853 W, respectively.

As shown in the Table III, the main and secondary copper losses of the designed model are larger than those of the prototype. It is because the main current and the conductor bar resistance of the former are larger than those of the latter.

As the results, while the total copper loss and the efficiency of the prototype are 83.23 W and 91.11 %, respectively, those of the designed model are 90.25 W and 90.43 W, respectively. The iron loss is ignored.

V. DESIGN AND ANALYSIS RESULTS

Table IV is the experimental results of the starting performance of the compressor during starting period.

In the table, there are three kinds of test conditions according to load of the compressor.

When the prototype is tested under the cooling condition, the motor is locked at certain position, though standard and overload conditions are satisfied. It is analyzed that the motor is locked at the initial starting positions which cause the negative starting torque in Fig. 12(a).

By contrast, the designed model can be started in the cooling condition as well as standard and overload conditions.

Table V summarizes the experimental results of the compressor at the steady-state when the torque is 2.20 Nm.

The efficiency of the designed model is increased by 2.7 % in comparison with the SPIM. Additionally, the losses except the winding copper loss of the designed model are remarkably reduced because the rotor joule loss is reduced.

The efficiency of the designed model by FE analysis in Table III is lower than that of the prototype. However, the experimental results are turned over. It is analyzed that the conductor bar resistance of the prototype is larger than that of the designed model when the motors are manufactured.

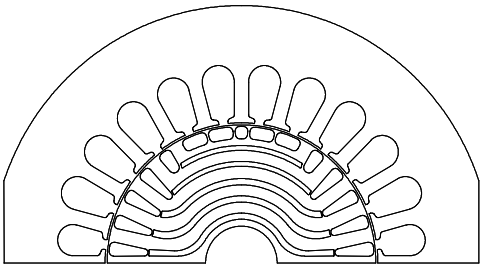

(a) Prototype

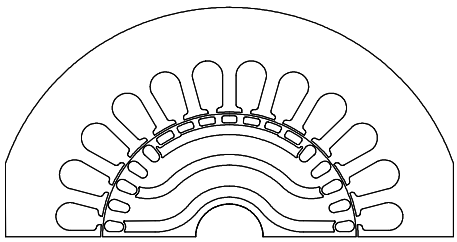

(b) Designed model

Figure 10. Cross-section of the prototype and the designed model of the LSynRM

TABLE II. BRIEF SPECIFICATIONS OF THE DESIGNED LSYNRM

Item		Prototype	Designed model
Input voltage (V) / Frequency(Hz)		115 / 60	
Winding		The series turns of main winding is 139 The series turns of auxiliary winding is 180 The winding ratio is 1.36	
Stator		The ratio of the inner diameter and the outer diameter is 0.54	
Rotor	The number of conductor bars	30	34
	The resistance of conductor bars (%)	100	152
	The number of flux barriers	5	3
	k_w	0.67	0.74

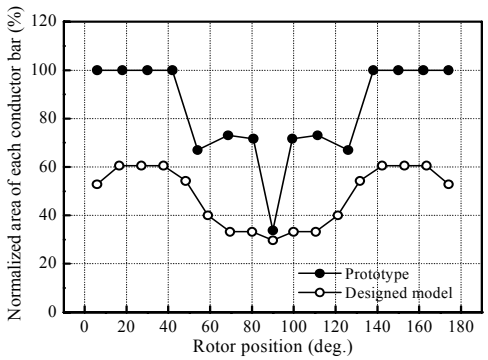

Figure 11. Normalized area of each conductor bars

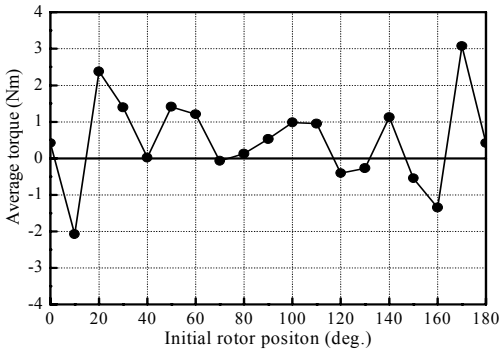

(a) Prototype

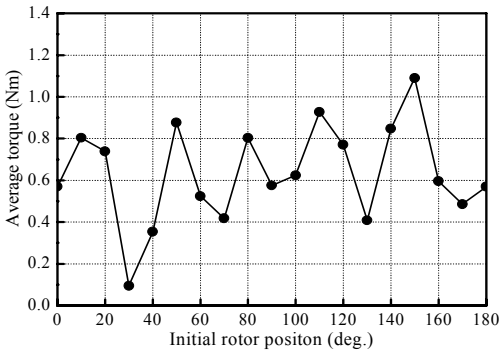

(b) Designed model

Figure 12. Analysis results of the average starting torque of the prototype and the designed model.

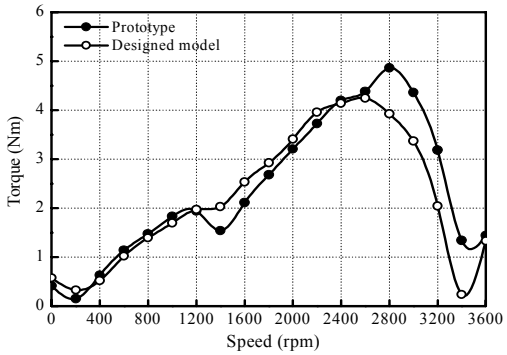

Figure 13. Average torques of the prototype and the designed model during starting period.

TABLE III. ANALYSIS RESULTS AT THE STEADY-STATE

Items		Prototype	Designed model
Rated torque (Nm)		2.26	2.26
Rated speed (rpm)		3,600	3,600
Rated output power (W)		853	853
Line current (A)		11.3	10.8
Main current (A)		7.41	7.66
Auxiliary current (A)		4.13	4.10
Efficiency (%) (Iron loss is ignored)		91.11	90.43
Copper loss	Main	42.28	45.18
	Auxiliary	30.53	30.09
	Secondary	10.42	14.98
Total copper loss (W)		83.23	90.25
Maximum reluctance torque(Nm)		4.87	4.24

TABLE IV. EXPERIMENTAL RESULTS OF THE STARTING PERFORMANCE

Item	Prototype	Designed model
Standard condition	Success	Success
Overload condition	Success	Success
Cooling condition	***Failure at certain position***	Success

TABLE V. STEADY-STATE EXPERIMENTAL RESULTS OF THE COMPRESSOR

Item	SPIM	Prototype	Designed model
Torque (Nm)	2.17	2.18	2.23
Speed (rpm)	3434	3600	3600
Power factor (%)	96.8	93.9	96.0
Efficiency (%)	84.3	85.2	87.0
1st copper loss (W)	62.0	92.0	82.0
Total loss (W) -1st copper loss (W)	83.4	50.7	43.6
Input power (W)	925.9	964.5	966.2

VI. CONCLUSIONS

This paper deals with the LSynRM design to improve starting performance for household appliances.

From the starting torque analysis results with the number of conductor bars, the number of 34 conductor bars is chosen for the LsynRM. In addition, the shape of the bar is decided to obtain the starting torque with the initial starting position.

By experimental results of the starting performance, It is confirmed that the designed model has a good self-start capability.

In addition, it is verified that the efficiency of the designed LSynRM is increased by 2.7 % in comparison with the SPIM in the steady-state

ACKNOWLEDGMENT

This work was financially supported by MOCIE through IERC program, Korea.

REFERENCES

[1] H. Murakami, Y. Honda, H. Kiriyama, S. Morimoto, and Y. Takeda, "The performance camparison of SPMSM, IPMSM and SynRM in use as air-conditioning compressor," *in Conf. Rec. the 34th IAS Annual Meeting*, vol. 2, pp. 840-845, Oct.1999.

[2] H. Nam, K. H. Ha, J. J. Lee, J. P. Hong, and G. H. Kang, "A study on iron loss analysis method considering the harmonics of the flux density waveforms using iron loss curves tested on Epstein samples," *IEEE Trans. Magn*., vol.39, no.3, pp. 1472-1475, May 2003.

[3] A. M. Knight, and C.I. McClay, "The design of high-efficiency line-start motors," *in Conf. Rec. the 34th IAS Annual Meeting*, vol. 1, pp. 516-522, Oct.1999.

[4] G. H. Kang, J. Hur, H. Nam, J. P. Hong, and G. T. Kim, "Analysis of Irreversible Magnet Demagnetization in Line-Start Motors based on Finite Element Method," *IEEE Trans. Magn*., vol.39, no.3, pp. 1488-1491, May 2003.

[5] I. Boldea, Z. X. Fu, and S. A. Nasar, "Performance evaluation of axially-laminated anisotropic (ALA) rotor reluctance synchronous motors," *IEEE Trans .Ind. Applicat.*, vol.30, no.4, pp. 977-985, July/August 2003.

[6] H. Kiriyama, S. Kawano, Y. Honda, T. Higaki, S. Moromoto, and Y. Takeda, "High performance synchronous reluctance motor with multi-flux barrier for the appliance industry," *in Conf. Rec. the 33th IAS Annual Meeting*, vol. 1, pp. 111-117, Oct.1998.